Calhoun: The NPS Institutional Archive
DSpace Repository

Theses and Dissertations 1. Thesis and Dissertation Collection, all items

1961-05-01

Experimental investigation of the ignition process of solid propellants in a practical motor configuration.

Lancaster, Robert W.

Princeton University

http://hdl.handle.net/10945/12165

Downloaded from NPS Archive: Calhoun

Calhoun is the Naval Postgraduate School's public access digital repository for research materials and institutional publications created by the NPS community. Calhoun is named for Professor of Mathematics Guy K. Calhoun, NPS's first appointed -- and published -- scholarly author.

Dudley Knox Library / Naval Postgraduate School
411 Dyer Road / 1 University Circle
Monterey, California USA 93943

http://www.nps.edu/library

NPS ARCHIVE
1961
LANCASTER, R.

EXPERIMENTAL INVESTIGATION OF THE IGNITION PROCESS OF SOLID PROPELLANTS IN A PRACTICAL MOTOR CONFIGURATION

ROBERT W. LANCASTER

LIBRARY
U.S. NAVAL POSTGRADUATE SCHOOL
MONTEREY, CALIFORNIA

m 91

EXPERIMENTAL INVESTIGATION
OF THE
IGNITION PROCESS OF SOLID PROPELLANTS
IN A
PRACTICAL MOTOR CONFIGURATION

by

LT. ROBERT W. LANCASTER, USN

Submitted in partial fulfillment
of the requirements for
the degree of Master of Science in Engineering
from Princeton University, 1961.

Signature of Author

ol
NCASTER ?

Library
U. S. Naval Postgraduate School
Monterey, California

ACKNOWLEDGMENTS

The author wishes to acknowledge the following persons and organizations whose collaboration made this work possible.

First and foremost, the author wishes to acknowledge especially the assistance of Professor Martin Summerfield who proposed this research. Professor Summerfield took an extremely active interest in the particular research study reported herein. The numerous discussions with him greatly aided the investigation, and his interest and encouragement during the research program were invaluable.

During the experimental program the author had occasion to confer with or receive invaluable assistance from practically every member of the Jet Propulsion Research Staff of the Department of Aeronautical Engineering. For their numerous contributions to the research project, the author wishes to express appreciation for the help afforded by Dr. Kimball P. Hall and Dr. Robert F. McAlevy, Research Associates.

Thanks are due also to Mr. Harold E. Burkert for his assistance and cooperation in the design and procurement of the experimental apparatus; to Messrs. Robert C. Knauer and Howland B. Jones for their aid with the electrical instrumentation; to Mr. Chris Felsheim, project technician, for his able and enthusiastic assistance in the fabrication and modification of experimental equipment; and to Mr. Keith C. Donaldson for

his competant assistance in the preparation of photographs for this report.

Finally, the financial support of the United States Air Force, Office of Scientific Research, that made the present investigation possible is acknowledged.

ABSTRACT

A study of the ignition process of a composite solid propellant was made in a combustion chamber whose configuration resembled that of a practical solid propellant motor. A small gas rocket chamber generated high temperature gaseous products, which in turn supplied the ignition energy to the internal surface of a cylindrical thin-web, case-bonded solid propellant grain.

The ignition delay--the time between ignition of the gas igniter and the first ignition of the solid propellant grain--was measured as a function of the temperature, pressure, the chemical reactivity of the hot gases, and the velocity of these gases over the solid propellant surface.

The ignition times were measured by means of a strain-gage pressure transducer inserted in the solid propellant motor chamber. By use of a direct writing oscillograph, a pressure-time trace of the transient ignition process is obtained. The ignition delay time was deduced from the shape of the pressure-time trace.

For the composite solid propellant (composition by weight: 80% NH_4ClO_4 plus 20% P-13 resin and additives), values for the ignition delay time, τ , ranged from 4.5 to 40 milliseconds, depending upon the mass velocity of the igniter gas in the solid propellant cavity. (This can be expressed equally well as an inverse dependence of τ on the product of "dummy chamber pressure" and mean gas velocity.) For constant igniter

gas composition, the data fitted the empirical relationship $\sqrt{\tau} \propto \dot{q}^{-1.025}$, where $\dot{q}$ is the heat flux input during the interval of exposure. This result, derivable from transient heating theory, suggests that for constant igniter composition the ignition delay is simply the time required for the attainment of a particular surface temperature at which the incipient reaction runs away.

An examination of the linear pyrolysis rates for P-13 resin and ammonium perchlorate also suggests that the attainment of a particular surface temperature is necessary to obtain a combustible mixture of solid propellant vapors adjacent to the propellant surface. Since the linear pyrolysis rate of the fuel is greater than that of ammonium perchlorate at low surface temperatures, the critical surface temperature at the instant of ignition should be strongly dependent upon the quantity of free oxygen present in the igniter gases. Since this series of tests was made with constant igniter composition, these tests do not differentiate between the theories of solid and gas phase ignition.

The motor configuration used in these experiments is not only a useful one for the study of the ignition process from a theoretical point of view, but it should have a great value as well in making an empirical analysis to determine the optimum ignition input for any particular propellant. The effects of the various ignition parameters on the flame spread time as well as on the ignition delay can be observed from the pressure-time trace.

TABLE OF CONTENTS

	Page
TITLE PAGE	i
ACKNOWLEDGMENTS	ii
ABSTRACT	iv
TABLE OF CONTENTS	vi
LIST OF FIGURES	vii
CHAPTER I: INTRODUCTION	1
CHAPTER II: EXPERIMENTAL APPARATUS	4
1. Introduction	4
2. The Solid Propellant Motor and Gas Rocket Igniter	6
3. Ignition System for Gas Rocket	11
4. Safety Disc	11
5. Gas Feed System	12
6. Instrumentation	13
CHAPTER III: IGNITER INPUT	15
CHAPTER IV: EXPERIMENTAL RESULTS AND DISCUSSION	18
CHAPTER V: CONCLUSIONS	22
CHAPTER VI: RECOMMENDATIONS FOR FUTURE RESEARCH	23
REFERENCES	25
TABLE	26
APPENDIX A: PROPELLANT AND INHIBITOR COMPOSITION	A-1
B: MANUFACTURE OF SOLID PROPELLANT GRAIN	B-1
C: COMMERCIAL EQUIPMENT AND MATERIAL	C-1
FIGURES	

LIST OF FIGURES

Figure

1. Rocket Motor for Study of Gaseous Ignition of Solid Propellant

2. Interpretation of Idealized Ignition Record

3. Solid Propellant Case-Bonded Grain

4. Exploded View of Motor Components

5. Circuit Diagram for Spark Ignition of Gas Igniter

6. Modified Spark Plug

7. Voltage-Time Trace of Spark Plug Gap

8. Flow Circuits for Igniter Gaseous Combustibles and Transducer Cooling Water

9. Strain-gage type, water-cooled, pressure transducer (Dynisco Corp)

10. Sectional View of Pressure Transducer

11. Circuit for Strain-Gage Instrumentation

12. Dead Weight Calibration of Pressure Transducer

13. Static Pressure Calibration of Instrumentation System

14. Ignition Pressure-Time Traces Showing Ignition Delay

15. Plot of "Dummy Chamber Pressure" Verses Ignition Time Delay

16. Plot of Ignition Time Delay Verses Average Heat Flux

17. Linear Pyrolysis Rate Curves for P-13 Resin and Ammonium Perchlorate

18. Solid Propellant Mold

19. Solid Propellant Casting Apparatus

CHAPTER I

INTRODUCTION

During the ignition of an operational solid propellant rocket motor, the surface of the solid propellant grain is subjected simultaneously to a complicated combination of conductive, convective, and radiative heat transfer, as well as attack by active chemical species released during the burning of the igniter charge. This exposure is much too complicated to be examined theoretically. However, each of these stimuli can be separately studied by means of suitable controlled ignition experiments (References 1, 2, and 3). Based on the results of various ignition studies several authors--notably a group at Chattanooga University (Reference 4) and later workers at the University of Michigan (Reference 5) and at Stanford Research Institute (Reference 3)--conjectured that the ignition process occurred in the gas phase rather than in the solid phase, as most commonly believed. Soon thereafter, the group at Princeton University developed the gas phase ignition theory (the runaway reaction occurring in the gas phase) and quantitatively correlated their experimental results with the predictions of the theory (Reference 1). Prior to the development of the gas phase ignition theory, correlations had been made with limited success on the hypothesis that ignition takes place when the surface temperature reaches a sufficient level to stimulate a critical rate of exothermic heat generation in the solid phase. This theory was developed in its most complete form by Hicks (Reference 6). In the

light of recent ignition research, however, it is apparent that the ignition mechanism cannot be completely described by the solid phase concept.

With the advent of large solid propellant rocket motors it is no longer economical to develop a suitable ignition system in a full scale motor. Therefore, a laboratory study of controlled ignition of solid propellant grains in a small practical motor configuration was needed to determine whether the ignition mechanism proposed in the gas phase ignition theory is applicable to a rocket motor configuration.

In the above-referenced shock tube studies at Princeton University, which led to the quantitative development of the gas phase ignition theory, the response of a propellant to a suddenly applied conductive heating exposure resulted in an ignition delay (the interval between the start of heating and the generation of the incipient flame) which decreased as the temperature, pressure, and chemical reactivity levels, respectively, of the heating gas were increased.

In an operational motor, the propellant charge is also exposed to a gas whose temperature, pressure, and chemical reactivity level can be varied experimentally.* In the present test motor, the hot gases consist of combustion products from

---

*Of course, in the practical motor other ignition stimuli may also be present, such as hot radiating solid or liquid particles. In some cases, there may even be vaporized metal oxides or inorganic salts, which introduce heat by condensing on the propellant surface.

a gas rocket ignition system in which a gaseous fuel is burned with various mixtures of oxygen and nitrogen. The combustion products then flow over the exposed propellant surface producing ignition primarily by convective heating.

A gas rocket ignition system was selected as the ignition stimulus because such a system offers broad and ready flexibility in the selection of closely controllable ignition parameters, and because it produces primarily a convective heating situation. Parameters capable of independent variation in a scheme of this sort include (1) the chemical reactivity of the ignition gases, (2) the "dummy chamber pressure" (the pressure of the gases in contact with the propellant prior to ignition of the propellant), (3) the temperature of the igniting gases, (4) the gas velocity past the propellant surface, and (5) the propellant composition.

CHAPTER II

EXPERIMENTAL APPARATUS

1. Introduction

The configuration of the test apparatus for these studies resembles that of a typical practical rocket engine utilizing an ignition system of the so-called Pyrogen type (Figure 1). Hot gases to supply the ignition stimulus emerge from the nozzle of a small gas rocket motor located at the head end of the solid propellant chamber. The hot exhaust gases then pass through the port of an internal burning case-bonded propellant grain (subjecting the latter primarily to convective heating) and emerge from the chamber through a final downstream nozzle. However, in the practical rocket a special solid propellant igniter grain burns in the Pyrogen chamber to supply the igniting hot gas. Hence, in the ignition test apparatus the gas rocket motor is performing as a "controllable Pyrogen" igniter.

The gas rocket burns methane, oxygen, and in some cases, diluent nitrogen. Propellant to be tested is fabricated in the form of a hollow thin-web cylindrical grain, and case-bonded to a thin-wall metal tube which is inserted into the motor casing. The ends of the grain are inhibited, allowing burning to occur only on the interior surface.

The overall ignition delay of the system consists of two principal parts, (1) the time necessary for the gas motor to ignite and fill the port of the solid propellant motor with a flowing stream of test gas at the pre-selected levels of

temperature, pressure, and chemical reactivity, and (2) the time required for the surface of the solid propellant to respond to this exposure by igniting and injecting its combustion products into the stream. An idealized pressure history of these events is sketched in Figure 2. When the methane and oxygen are injected into the gas rocket, ignition of the combustible mixture increases the pressure to the "dummy chamber pressure" level where it remains until the solid propellant grain is ignited. The principal experimental objective of this research is measurement of the duration between the ignition of the gas igniter and the ignition of the solid propellant test sample. This time interval is defined as the ignition delay of the solid propellant. The ignition delay for a series of propellant formulations is measured as a function of the temperature, pressure, and chemical reactivity level of the hot gas, and as a function of the flow velocity of this gas over the propellant surface.

The mass flow rate of gas through the two rocket chambers before ignition of the solid propellant grain is controlled by means of an impingement injector containing critical-flow(choked) orifices for the fuel and oxidizer feed systems. The temperature and chemical reactivity level of the burnt gas depends primarily on the relative proportions of methane, oxygen and nitrogen injected into the gas rocket, with a slight dependence on the combustion pressure resulting from the suppression of

dissociation as the combustion pressure is increased. For any given combination of mass flow rates of these gases, the combustion pressure ("dummy chamber pressure") level is fixed by the throat area of the solid propellant exhaust nozzle (the gas rocket exhaust nozzle is designed so that it will always be unchoked).

Finally, once these conditions are established, the flow velocity of the hot gas through the port of the solid propellant grain is a function of only the port diameter and nozzle throat diameter. A wide range of exposure conditions is available simply by selecting the appropriate combination of mass flow rates of the gases, the composition of the gas mixture, the throat diameter of the exhaust nozzle, and the port diameter of the test sample.

2. The Solid Propellant Motor and the Gas Rocket Igniter

The small solid propellant rocket motor with a gas rocket providing the ignition energy required a system possessing a minimum L^*. This design criterion is necessary to provide a minimum "rise time" of the chamber pressure before solid propellant ignition to the operating "dummy chamber pressure" (the ideal igniter input would be a step function) and to permit detection of the first instant of solid propellant ignition by a sharp increase in pressure due to increased mass flow. A "dummy chamber pressure" range of operation between

[illegible] and [illegible] psia was desired.**

The flow conditions assumed to exist in the system are based on calculations that assume isentropic flow of an ideal gas through the exhaust nozzle and the port, and adiabatic complete combustion.

The exit nozzle determines the solid propellant grain surface area for a given chamber pressure, as well as the mass flow of igniter gases, which in turn establishes the desired "dummy chamber pressure." A nozzle throat diameter of 0.25 inches was found to provide a minimum L^* for the system.*** The inter-nozzle through which the igniter

---

**The original concept also involved fixing the flow rate through the gaseous igniter by critical orifices in the gas feed lines just upstream of the injector, thereby maintaining positive gas flow throughout the burning of the solid propellant. Because of the upper pressure limitations of the gas source, the high costs of manufacturing a number of injectors to provide the desired range of operation was not feasible, since it was not known whether such a system would be suitable for ignition studies. The desired range of igniter operation could be achieved by metering the gas just upstream of the injector with interchangeable critical orifices, at a relatively low cost.

However, operation of the equipment showed that the ignition characteristics of the gaseous mixture were more desirable when metering occurred at the injector orifices. This will be discussed in detail in a later section. Although the experimental apparatus is described in its present configuration, in some instances the component design would have changed slightly to provide an optimum L^* had the system been designed for metering at the injector.

***Because of the very low methane mass flow rates required at the lower limit of the operating range, the small size of the methane metering orifice became the controlling factor in establishing a minimum L^* for the system. This exit diameter required a methane metering orifice for the lower limit of operation slightly greater than the minimum size that could be manufactured without excessive costs.

gases pass into the solid propellant grain cavity has a diameter of 0.30 inches. This nozzle size provided a tolerable small pressure drop between the gas igniter and solid propellant chambers and yet is sufficiently small to direct the gases axially into the solid propellant cavity. This nozzle is unchoked at all times during a firing operation.

The impingement injector was designed to be critical until after ignition of the solid propellant grain, so that the initial pressure rise caused by ignition of the igniter gases and the chamber pressure rise due to an increased mass flow when ignition of the solid propellant grain commences would not be felt in the gas lines. This degree of choking of the injector orifices is necessary to maintain a minimum L^* for the system until after ignition of the solid propellant grain has commenced. Four pairs of impingement orifices are spaced 90° apart on the face of the injector. The angles of the orifices are such that after impingement the flow is axial. Each impingement point is 0.1250 inches from the face of the injector and 0.375 inches from the axis of the combustion chamber.

The gas igniter combustion chamber is 1.25 inches diameter and 2.0 inches long. Built into the chamber are openings for two spark plugs for ignition of the gas, a pressure transducer, and an over-pressure safety-disc connection.

The solid propellant grain is a hollow thin-web cylindrical grain, case-bonded to a thin-wall metal tube

which is inserted into another cylindrical tube that comprises the motor casing. The ends of the grain are inhibited, allowing burning to occur only on the interior surface.

The solid propellant grain port diameter was selected to be 0.75 inches, resulting in a 9-to-1 port-to-throat area ratio. A large area ratio was desired to keep the convective heat transfer coefficient at a low value to insure an ignition delay of sufficient length to be accurately measured. Also, it provided for a low L* and a relatively short grain. Neglecting the igniter gas flow, the solid propellant grain was designed to provide approximately 200 psia chamber pressure when the exposed surface was completely ignited. For an exit nozzle throat diameter of 0.25 inches (0.0490 sq.in.) and a burning surface to throat area ratio $K_n = 230$ (Reference 7), a burning surface of 11.25 sq.in. is required. For a port diameter of 0.75 inches (circumference = 2.36 inches), the grain length is 4.78 inches. Because an internal burning cylindrical grain burns progressively, and because of the necessity for a low L* system, the grain length was reduced to 3.75 inches. Also, the shorter grain greatly simplified the drilling of the grain port.

The grain ends are inhibited with 0.10 inches of P-13 resin inhibitor. The 4-inch long thin-wall tube extends slightly beyond the inhibited surface to permit the use of an O-ring seal between the inhibitor and the adjacent motor

port, to insure against hot gases seeping into any small cracks should any portion of the case-bond not hold. The thickness of the grain web is 0.25 inches and the grain weight is 88 grams. Figure 3 shows two photographs of the grain; the upper picture shows the grain as it appears after drilling the port, the lower picture shows a grain ready for insertion into the motor.

The manufacture and preparation of the grain for firing is discussed in detail in Appendix B.

In addition to the motor components mentioned above, a spacer to support the pressure transducer connection was inserted downstream of the solid propellant grain. The spacer has the same inside diameter as the solid propellant grain prior to burning.

The internal volume (V) of the motor system is 5.17 cu.in. resulting in an $L^* = \frac{V}{A_t} = 105$ inches. Since the fuel and oxidizer pass through the injector as gases, and assuming that combustion occurs near the injector surface, the combustion gases stay a certain time, τ_{tr} , within the system until combustion is complete. This residence time can be represented by $\tau = \frac{1}{\Gamma^2} \frac{L^*}{C^*}$ where $\Gamma = \sqrt{\gamma} \left(\frac{2}{\gamma+1} \right)^{\frac{\gamma+1}{2(\gamma-1)}}$.
For $\gamma = 1.2$ and a characteristic velocity, $C^* = 4500$ ft/sec, the residence or rise time (assuming ignition at the instant the gases are injected into the combustion chamber) is calculated to be 5.65 milliseconds.

Components of the motor which must withstand high temperatures are fabricated from commercial copper, which acts

as an excellent heat sink and is relatively non-reactive to high concentrations of hot oxygen. The solid propellant section is made of stainless steel designed for a burst pressure of 3000 lbs. Brass was selected as the injector composition because of its machinibility. Figure 4 shows an exploded view of the solid propellant motor and gas rocket igniter.

3. Ignition System for the Gas Rocket

Two spark plugs were mounted in the gas rocket chamber for ignition of the methane-oxygen mixture. A 110 volts AC neon transformer rated at (450 VA capacity, Sec 15,000 V, 30 ma) provided the excitation energy for the spark. The secondary is center-grounded providing 7500 volts to each spark plug. The ignition system wiring circuit is shown in Figure 5. To prevent welding of the electrodes, the spark plugs were modified (Figure 6) by cutting off the side electrode. With this extended gap, the spark is seen to rotate about the end of the plug. Figure 7 is an oscillograph trace of the spark voltage in air during 1/2 cycle of a 60 cycle sine wave input. The duration of the spark is approximately 95% of the half-cycle time. A spark system which approached a continuous spark was necessary to insure ignition of the gas without delay, as soon as a combustible mixture entered the combustion chamber.

4. Safety Disc

A pressure burst disc was installed in the igniter chamber to protect the motor and instrumentation from

excessive over-pressure. Fuller RL 3700 compound was inserted in the extension between the burst disc and the combustion chamber wall to protect the disc from the hot gases. Hydrostatic tests showed that the presence of the compound did not affect the burst pressure of the disc.

5. The Gas Feed System

Figure 8 shows a flow circuit of the gas feed system. Two Marotta PV-20-F pneumatic actuated on-off valves placed in the gas feed lines as close to the injector as possible provide simultaneous flow of the fuel and oxidizer to the injector. The pressure of the gas feed system is controlled by two Grove RBX-204-015 5-1500 pressure regulators. Two 0-2000 lbs. Heise pressure gages provide gas feed pressure measurements from taps in the feed lines just upstream of the on-off valves. Since the gas velocity is small in the feed lines, the static pressure is approximately equal to the total pressure. Therefore, no pressure correction is required to obtain the proper mass flow. The gas feed system is constructed with 1/2-inch stainless steel tubing.

Check valves are inserted in the feed lines between the on-off valves and the injector to prevent any reverse flow in the feed system. During burning of the solid propellant the motor pressure exceeds the gas feed line pressures which necessitates the use of check valves to prevent the hot combustion gases from entering the feed system.

A nitrogen purge system is used to purge the motor of any combustible gases before each firing.

c. Instrumentation

The sensing instrument consists of one Dynisco strain-gage water-cooled pressure transducer (Figure 9) located aft of the solid propellant grain, to sense the pressure in the solid propellant grain cavity. Figure 10 shows the sectional view of the pressure transducer. By use of a Minneapolis-Honeywell Visicorder 906B direct-writing oscillograph, a pressure-time trace of the ignition process is obtained. The instrumentation system provides a measurement of the delays encountered during the ignition process within one millisecond accuracy. Specifically, the following delays were measured: (1) the time to obtain the "dummy chamber pressure" and (2) the time to ignite the solid propellant.

The signal produced by the transducer is amplified by an AccuData III Wide Band Differential D-C Amplifier which is a chopper-stabilized all-transistor D-C amplifier. Under all over-load conditions, less than 100 ma is produced at the amplifier output, which provides positive protection for the fluid-damped galvanometers used in the Minneapolis-Honeywell Visicorder.

The galvanometer is fluid-damped with a flat frequency response of 0-2000 cps. The maximum peak-to-peak deflection with ± 2% linearity is 6 inches.

A strain-gage balance and negative bias system is shown in an instrumentation wiring schematic in Figure 11. The negative bias input to the amplifier off-sets the zero

of the galvanometer in the negative direction, permits greater amplification of the strain-gage input, and prevents the amplifier from saturating during the burning of the solid propellant grain. To provide a check prior to each run to determine whether the instrumentation system is functioning properly, a positive 13.5 mv gage output is obtained by use of a 50K resistor and a push button switch. This output is equivalent to 450 psig. If the system is operating properly, the galvanometer deflects a distance equal to that obtained during calibration of the system. A dead weight calibration of the pressure transducer is shown in Figure 12. A static pressure calibration of the instrumentation system is shown in Figure 13.

The Minneapolis-Honeywell Timing Unit is a self-contained multivibrator oscillator which supplies accurately spaced sharp pulses at intervals of 0.01, 0.1, and 1.0 seconds. The pulse characteristics are such that, with the timing signal applied to two 3300 cps natural frequency galvanometers, the pulsed galvanometer traces will meet in the center of the record providing full-width timing lines.

CHAPTER III

IGNITER INPUT

Initially, the igniter input was achieved by pre-flowing the cold igniter gases (metered by critical orifices upstream of the injector) through the motor to permit the gas flow to stabilize prior to energizing the spark. When the mixture of methane and oxygen ignited, exceedingly high pressures and pressure waves occurred in the chamber as a result of a constant volume explosion. The pressure decay time to the equilibrium pressure was large compared to the solid propellant ignition delay. The igniter input achieved by this method was unsatisfactory.

The results of the above tests indicated a continuous pre-spark was necessary to permit ignition of the gases as soon as a combustible mixture existed in the rocket chamber. Because of the appreciable filling time of the feed lines between the orifices and the injector, it was found that it was no longer feasible to use the critical orifices upstream of the injector. Since the injector orifices were choked until after ignition of the solid propellant, tests were made to determine the feasibility of using the injector orifices for metering of the gas input to the motor. The results of these tests showed: a reduced initial pressure at ignition, below that which would occur for constant volume combustion; no adverse pressure waves; and a small pressure decay time to the equilibrium pressure. This igniter input is considered satisfactory, although not ideal.

The nature of this starting transient is discussed in the following paragraphs. In analyzing the igniter input (Figure 14) it is observed that the ignition process of the igniter gases takes place in a time which is short compared to the steady-state "dwell time" of combustibles in the chamber. Therefore, the ignition process can be considered to take place at constant volume and fixed mass. $(P_c)_{cv_{eff}}$ is defined as the observed pressure of the hot gases at time $t = 0$.

Since the motor and the feed lines between the check valves and the injector are filled with nitrogen at atmospheric pressure prior to flow of the igniter gases, the exact proportions of fuel, oxidizer, and diluent (N_2) are not precisely known during the igniter transient. Therefore, the temperature of the flame propagating through this gas mixture of varying composition will not reach a steady-state value until the nitrogen has been displaced from the motor. However, the effective temperature at $t = 0$ can be defined as the one which would produce $(P_c)_{cv_{eff}}$ and can be expressed by

$$\left.\frac{P_c}{T_c}\right._{eff} = \frac{P_o}{T_o} .$$

During the adjustment time following the constant volume deflagration the composition of the gases in the chamber changes from that corresponding to ϕ_{eff} to ϕ_{design} which produces a change in the temperature of the chamber gas from $T_{f\ eff}$ to $T_{f\ design}$. The time to establish equilibrium conditions can be calculated by writing the continuity equation

in the following form for the entire combustion chamber

$$\frac{VM}{RT_c}\frac{dp}{dt} = \dot{m}_{in} - \frac{\Gamma\sqrt{g}\,PA_t}{\sqrt{\frac{R}{M}T_c}}$$

where V is the volume of the combustion chamber, M is the molecular weight of the gas, R is the universal gas constant, $\dot{m}$ is the input mass flow, and g is the gravitational constant.

Assuming T_c = constant and integrating for the boundary condition $P = P_{eff}$ at $t = 0$, the time constant for the adjustment period is

$$\frac{V}{A_t}\frac{1}{\sqrt{\frac{R}{M}T_c}}\frac{1}{\Gamma}$$

which is equivalent to the steady-state stay time of the gas in the chamber since $\tau_{tr} = \frac{1}{\Gamma^2}\frac{L^*}{C^*}$ where $\frac{V}{A_t} = L^*$ and $\frac{1}{\sqrt{\frac{R}{M}T_c}} = \frac{1}{\Gamma C^*}$. But since the flame temperature varies during the decay time, there exists a continuously changing residence time during the transient period.

During this adjustment period, there exists a pressure greater than the equilibrium pressure and a temperature less than the equilibrium temperature. Although the heat flux is influenced by both pressure and temperature, the effects tend to cancel one another, resulting in a heat flux approximately equal to the equilibrium heat flux. The results suggest that this igniter transient introduced negligible error in the range of the ignition delay time between 4.5 and 40 milliseconds.

CHAPTER IV

EXPERIMENTAL RESULTS AND DISCUSSION

The effect of pressure or mass velocity of the hot igniter gases of constant composition on the ignition delay of a series of solid propellant grains was measured. The experimental results are tabulated in Table I and plotted in Figure 15.

The composition of the igniter gases before combustion in the gas rocket was $CH_4 + 1.88\ O_2$. Assuming the igniter combustion efficiency is constant from run to run and the products of combustion due to dissociation only vary slightly over the "dummy pressure" range tested (2 to 7 atm), the flame temperature is essentially constant from run to run. The initial temperature of the solid propellant is maintained the same from run to run, and assuming the $\overline{T}_w$ (the mean temperature of the solid propellant surface during the ignition time delay) is constant from run to run; the convective heat flux $\frac{d\overline{q}}{dt} = h_c\ (T_g - \overline{T}_w)$ can be assumed independent of the ΔT , since $(T_g - \overline{T}_w)$ is so large compared with a small change of T_g , where T_g is the temperature of the hot gases. Therefore, the primary experimental parameter which affects the heat flux is the convective heat transfer coefficient.

For turbulent flow, h_c is correlated with the properties of the fluid and the configuration of the flow

channel by the relation

$$\frac{h_c D}{k} = 0.023\left(\frac{DG}{\mu}\right)^{0.8}\left(\frac{C_p \mu}{k}\right)^{0.4}$$

in which D is the effective diameter of the flow channel, h_c is the convective heat transfer coefficient, k is the thermal conductivity of the hot gases, G is the mass velocity, μ is the viscosity, and C_p is the specific heat of the gases. For constant igniter composition the above can be reduced to

$$h_c = \text{constant}\,\frac{G^{0.8}}{D^{0.2}}$$

With the above restrictions on $\overline{T}_w$ and T_g, the heat flux remains essentially constant during the pre-ignition interval for a given mass velocity through the solid propellant grain port. The exact values of the heat flux ($\dot{q} \equiv \frac{dq}{dt} = h_c[T_g - \overline{T}_w]$) cannot be calculated (the value of μ, k, C_p, and ΔT are not known exactly); however, a relative heat flux, $\dot{q}/\dot{q}_o$, can be calculated since the only variable is mass velocity. These values are tabulated in Table I.

It has been pointed out by Ryan (Reference 2) from elementary theory of transient surface heating that the ignition delay can be expressed by $1/2 \ln \tau = \text{constant} - \ln \dot{q}$, if the ignition delay is based upon the attainment of a particular surface temperature at the instant of ignition. The experimental results shown in Figure 16 show the time delay as a function of a relative $\dot{q}$. For constant igniter

composition, the data fitted the empirical relationship $\sqrt{\tau} = \dot{q}_0^{-1.025}$, which corresponds very closely to that predicted by the heat transfer theory.

Since no excess oxygen was present in the hot igniter gases, all oxygen to support combustion of the solid propellant must come from the solid propellant itself. Therefore, the solid propellant surface must reach a temperature that is sufficiently high to permit a combustible concentration of fuel and oxidizer vapors to form in the adjacent gaseous layer before ignition can occur. The results of these tests imply that the surface temperature at the ignition instant is a constant for a given igniter composition. This result can also be predicted from the linear pyrolysis rates of P-13 resin and ammonium perchlorate which are shown in Figure 17. At low propellant surface temperatures, the linear pyrolysis rate of P-13 resin exceeds that of ammonium perchlorate. As the surface temperature increases with time, the pyrolysis rate of ammonium perchlorate increases at a faster rate than that of P-13 resin until a particular surface temperature is reached that produces a combustible mixture near the surface of the solid propellant at which time ignition occurs. Since no free oxygen was present in the igniter gases, it is postulated that the ignition surface temperature is slightly less than the temperature which produces equal pyrolysis rates for the two components of the propellant.

Since the small change in flame temperatures of the igniter gases resulting from the increased pressure of

combustion was not taken into account, the slight increase in the heat flux at the higher "dummy chamber pressures" would tend to make the slope of the curve in Figure 16 somewhat steeper than -1. That is, perhaps the higher exponent observed can be explained this way.

Since only one igniter composition was tested, these tests do not differentiate between the theories of solid and gas phase ignition.

CHAPTER V

CONCLUSIONS

As a result of the tests conducted, it is concluded that:

1. The motor configuration as used in these experiments is a useful tool for study of solid propellant ignition characteristics--not only from a theoretical point of view, but also from an empirical point of view, for determining the optimum ignition parameters for a given type of rocket. The effects of the various ignition parameters on the flame spread time as well as the ignition delay can be deduced from the pressure-time trace.

2. The ignition delay followed the relationship $\sqrt{\tau} = \dot{q}_0^{-1.025}$ for constant igniter composition, which suggests that to achieve ignition the surface temperature must be brought to a certain critical level.

3. Short ignition delays can be obtained by a high convective heat transfer coefficient.

4. This series of tests does not differentiate between the theories of solid and gas phase ignition.

CHAPTER VI

RECOMMENDATIONS FOR FUTURE RESEARCH

For future research, it is recommended that:

1. The adiabatic flame temperature of the igniter gases be reduced by increasing the oxidizer fuel ratio to produce longer ignition delays, which also will permit varying the oxygen content of the igniter oxidizer gas to determine the effect of excess oxygen on the ignition time delay.

2. The motor exit nozzle be sealed with a lightweight foil to permit the evacuation of the atmospheric air from the combustion chamber prior to firing. Therefore, only a small mass of gas would be present in the chamber when ignition of the methane-oxygen mixture occurred, which would possibly reduce or eliminate the pressure peak that was produced when the gas rocket ignited. Also the igniter gas composition would be known at all times since no diluent would be present in the motor. A nozzle seal that will burst or burn immediately after ignition of the igniter should be used.

3. The pyrolysis rates for P-13 resin and ammonium perchlorate be determined for the surface temperature range 400-700°K.

4. The surface temperature histories during the ignition process be measured for several different igniter energy inputs.

5. The gas rocket igniter be replaced by a solid propellant ignition system to better determine the ignition process as affected by a practical ignition system.

REFERENCES

1. McAlevy, R. F. III, Cowan, P. L., and Summerfield, M., "The Mechanism of Ignition of Composite Solid Propellants by Hot Gases," Solid Propellant Rocket Research, Vol. I of Progress in Astronautics and Rocketry, (Editor, M. Summerfield) Academic Press, New York, 1960, p.623.

2. Baer, A. D., and Ryan, N. W., "Fundamental Studies of Ignition by Means of a Shock Tube," Ibid., p.653.

3. Beyer, R. B., and Fishman, N., "Solid Propellant Ignition Studies with High Flux Radiation Energy as a Thermal Source," Ibid., p.673.

4. Gallagher, M., "Investigation of Possible Improvement in Rocket Ignition," Technical Report No.2, Industrial Research Institute, University of Chattanooga, 1 September 1953 (CONFIDENTIAL).

5. Churchill, S. W., Kruggel, R. W., Brier, J. C., "Ignition of Solid Propellants by Forced Convection," AICh.E. Journal, December, 1956, p.568.

6. Hicks, B. L., "Theory of Ignition Considered as a Thermal Reaction," J. Chem. Phys., Vol.22, No.3, March, 1954, p.414.

7. Hermance, C. E., "Comparison of Burning Rates of Solid Propellants in Strands and in Rocket Motors," Master's Thesis, Princeton University, June, 1961.

8. Bastress, E. K., "Modification of the Burning Rates of Ammonium Perchlorate Solid Propellants by Particle Size Control," Ph.D Thesis, Princeton University, January, 1961.

9. Chaiken, R. F., Anderson, W. H., "The Role of Binder in Composite Propellant Combustion," Solid Propellant Rocket Research, loc.cit., p.227.

10. Chaiken, R. F., Aerojet-General Corporation Personal Communication, January, 1960.

TABLE I

IGNITION TIME DELAY MEASUREMENTS

Run	Observed "Dummy Chamber Pressure" (psia)	Ignition Delay-τ (sec)	$\tau^{\frac{1}{2}}$	Relative Heat Flux
1	118	4.35	2.09	2.99
2	47	20.4	4.51	1.432
3	73	8.90	2.98	2.035
4	87	7.3	2.70	2.345
5	80	8.5	2.92	2.19
6	61	12.75	3.57	1.765
7	43	22.5	4.75	1.334
8	30	40.3	6.35	1

APPENDIX A

PROPELLANT AND INHIBITOR COMPOSITION

The compositions of the inhibitor and the propellant tested are outlined below. All propellant was manufactured in the solid propellant processing facilities of the Aeronautical Engineering Department, Princeton University, Princeton, New Jersey.

Propellant composition:

Ammonium Perchlorate (bimodal mix)	80.00%
Polystyrene Resin (Rohm and Haas P-13)	19.75%
Nuodex Cobalt	.10%
Lecithin B-60	.10%
Lupersol DDM	.05%

Inhibitor:

Polystyrene Resin (P-13)	96.618%
Nuodex Cobalt	.965%
Lecithin B-60	.965%
Lupersol DDM	1.450%

APPENDIX B

PREPARATION OF TEST GRAIN

A standard manufacturing process (Reference 8) was used in preparing the propellant for casting.

Figure 18 is an exploded view of the solid propellant mold. To cast the propellant the thin-wall tube is inserted into the base of the mold and placed in a vacuum desiccator (Figure 19). A vacuum of approximately 16 mm. of H_g is maintained in the desiccator during casting. The propellant is fed through a funnel with the feed rate being controlled by a thumb screw pinch clamp on a length of flexible tubing below the funnel. The propellant passes through a narrow slit in the end of the feed line entering the mold in the form of a thin continuous ribbon. This procedure eliminates air bubbles which may have been introduced during removal of the propellant from the mixer.

After removing the mold from the desiccator, the mandril (coated with a silicone high vacuum grease to allow easy removal) is inserted into the propellant. The base of the mold is tapered to provide centering of the mandril. Any excess propellant is removed prior to putting on the mold cap. Figure 16 shows the assembled mold.

The mold containing the propellant is placed in the oven at 80°C for 18 hours after which time the mandril is removed. The propellant is cured for an additional six hours without the mandril to insure that the propellant is properly cured near the center of the mold.

To prepare the ends of the grain for inhibiting, the grain is placed in the lathe for removal of propellant to a depth of 1/8" from each end of the metal casing. Approximately 0.10" of inhibitor is applied to one end of the grain. A greased tapered rubber stopper is inserted into the grain port to prevent the inhibitor from contacting the internal surface of the grain. After approximately one hour of curing at room temperature the inhibitor has solidified sufficiently to remove the stopper and repeat the procedure on the opposite end of the grain. By curing the inhibitor at room temperature a good bond to the propellant and the metal casing is obtained. Also the inhibitor remains slightly tacky and elastic permitting use of an O-ring seal at each end of the grain as a further safe guard against the presence of any lack of case-bonding. It was noted by microscopic examination of the case-bond of the grain to the metal tube that the propellant was not always 100% case-bonded.

After inhibiting the grain ends, the propellant is wrapped in aluminum foil, placed in containers containing silica gel and placed in the magazine for storage.

A few days prior to firing the grain is prepared for testing. By drilling on a lathe, the grain cavity is enlarged to 3/4" diameter in two steps: the first cut is made with a 11/16" counter bore, and a 3/4" counter bore is used for the second cut By drilling the grain port to 3/4" rather than casting the grain with a 3/4" port, any mold surface effects or contamination from the release agent,

is eliminated, and a uniform surface is produced on all grains.

The prepared grains are wrapped in aluminum foil, placed in a desiccator containing silica gel and kept at room temperature until placed in the motor for firing.

APPENDIX C

COMMERCIAL EQUIPMENT AND MATERIALS

1. Equipment

Item	Manufacturer or Supplier	Use
Pressure Transducer PT-49F-IM	Dynamic Instrument Co. Cambridge, Mass.	Chamber Pressure Measurement
Direct Writing Oscillograph 906 B	Minneapolis-Honeywell Union, N. J.	Pressure-Time Record
Timing Oscillator #101336	Minneapolis-Honeywell Union, N. J.	Time Lines for Visicorder Record
AccuData III Differential D-C Amplifier	Minneapolis-Honeywell Union, N. J.	Amplify Transducer Output
Pressure Gage #5351R, 0-2000 PSI	Heise Bourdon Tube Co. Newtown, Conn.	Gas Feed Pressure Measurement
Pressure Gage B-100, 0-100 PSI	Helicord Gage Division American Chain & Cable Co. Bridgeport, Conn	Water Pressure Gage
Safety Head and Rupture Disc	Black, Sivallo & Bryson, Inc. Wayne, Pa.	Safety for Motor Over Pressure
Neon Transformer 450 VA Capacity; Secondary 15000 V	Hutchinson Electric Co. Trenton, N. J.	Spark System
Water Pump	Labanco Pump Co. Bellemead, N. J.	Transducer Cooling
Electric Motor Type F-Z, 3/4 H.P. Single Phase 1725 RPM	Westinghouse Electric Supply Company Trenton, N. J.	Water Pump Motor
Counterbore Drills 11/16" and 3/4"	Sinclair Industrial Trenton, N. J.	Drill Propellant Port

Item	Manufacturer or Supplier	Use
Vacuum Disiccator P-1540 Pyrex	Scientific Glass Apparatus Co. Bloomfield, N. J.	Propellant Casting
Pyrex Funnel 60° #6220 GR28, 65 mm	Scientific Glass Apparatus Co. Bloomfield, N. J.	Propellant Casting
Stopper Neoprene No.8	Scientific Glass Apparatus Co. Bloomfield, N. J.	Propellant Casting
Screw Clamp C-4835, 5/8"x 1"	Scientific Glass Apparatus Co. Bloomfield, N. J.	Propellant Casting Feed Control
Dome Regulator Grove RBX-204-015	Herback & Rodman Inc. Philadelphia, Pa.	Fuel and Oxidizer Pressure Control
Pressure Reducing Regulator Model 15H	Grove Regulator Co. Oakland, Calif.	Dome Regulator Control
Pressure Gage 0-3000 PSI 2" Face	Truesdall Co. Princeton, N. J.	Fuel and Oxidizer Supply Press
Check Valve K-1253-4	Kohler Company Newark, N. J.	Prevent Reverse Flow in Gas Fuel System
Check Valve No. P6-615	Circle Seal Prod. Co., Inc. Philadelphia, Pa.	Prevent Reverse Flow in Gas Feed System
Pneumatic Valve Marotta PV-20-F	Marotta Valve Corp. Taylor, N. J.	Gas Flow On-Off Valve
Solenoid Valve Marotta MV 74	Marotta Valve Corp. Taylor, N. J.	Pneumatic Valve Control
Spark Plugs Champion N-5	Prince Motor Parts Princeton, N. J.	Ignition of Gas Rocket
Toggle Switch, S.P.S.T. Cutler-Hammer No.ST 42A	H. L. Dalis Co. Long Island, N. Y.	Electric Circuit Switches

2. Materials

Item	Manufacturer or Supplier	Use
Methane (C.P.) 240 cu.ft. 2000 PSI	The Metheson Co., Inc. E. Rutherford, N. J.	Igniter Fuel
Oxygen-Nitrogen 1 A Cylinder 2000 PSI	Air Products Islen, N. J.	Igniter Oxidizer
Oxygen Electrolytic 99% Pure	General Dynamics Co. Liquid Carbonic Div. Harrison, N. J.	Igniter Oxidizer
Nitrogen	Linde Air Products Linden, N. J.	Control Press and Motor Purge
Visicorder Recording Paper Spec 2 Extra Thin	Eastman Kodak Co. Rochester, N. Y.	Pressure-Time Record
Ammonium Perchlorate Standard AMS-C66F	American Potash Co. New York, N. Y.	Propellant Oxidizer
Polyester Resin P-13	Rohm & Haas Co. Philadelphia, Pa.	Fuel Binder
Lupersol DDM	Wallace & Tierman Buffalo, N. Y.	Propellant Curing Agent
Nuodex Cobalt Accelerator	Nuodex Products Co. New York, N. Y.	Propellant Curing Agent
Lecithin, Vegetable Technical	Fisher Scientific Co. Fair Lawn, N. J.	Propellant Wetting Agent
"O" Ring Linear #11-226	Linear, Inc. Philadelphia, Pa.	Motor Pressure Seals
"O" Ring Linear #11-111	Linear, Inc. Philadelphia, Pa.	AN Fitting Pressure Seals
"O" Ring Linear #11-112	Linear, Inc. Philadelphia, Pa.	AN Fitting Pressure Seals
"O" Ring Linear #11-214	Linear, Inc. Philadelphia, Pa.	Propellant Grain End Seals

Item	Manufacturer or Supplier	Use
Stainless Steel RD 3-1/2 Dia Type 316	Whitehead Metals Inc. Harrison, N. J.	Solid Propellant Motor Casing Flange
Copper Bar Round 3-1/2" Dia	Philadelphia Bronze & Brass Co. Philadelphia 21, Pa.	Motor Components
Stainless Steel Tubing Seamless Type Box 1-3/8" O.D. x .065"	A. B. Murray Elizabeth, N. J.	Solid Propellant Casing
Brass Bar Round 3-1/2" Dia	Philadelphia Bronze & Brass Co. Philadelphia 21, Pa.	Injector Assembly
Stainless Steel Type 304 - Seamless 1.375" O.D. .065" Wall	A. B. Murray Elizabeth, N. J.	Casing for Propellant Grain
Stainless Steel Type 304 Seamless 1/2" O.D.x.035" Wall 1/4" O.D.x.035" Wall	David Smith Steel Co. South Plainfield, N. J.	Gas Feed System Piping
AN Fittings Stainless Steel	Dee Aircraft Alberson, Long Island, N. Y.	Tubing Connectors
High Vacuum Grease Silicone	Dow Corning Corp. Midland, Mich.	Mold Release Agent
Alum Bar Rd. 2" Dia Type 6061-T6	Whitehead Metals, Inc. Harrison, N. J.	Solid Propellant Mold Base and Cap
Alum Bar Rd. 5/8" Dia Type 6061-T6	Whitehead Metals, Inc. Harrison, N. J.	Mold Mandril

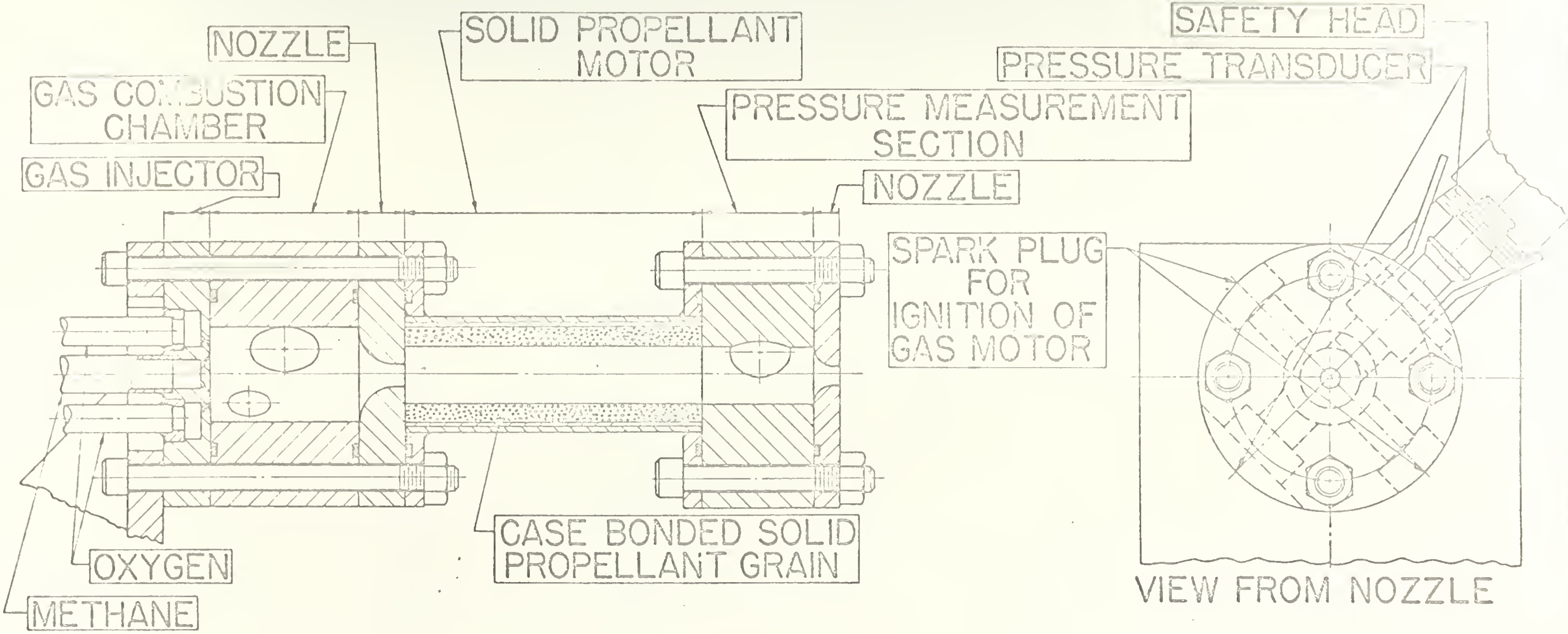
NOZZLE
GAS COMBUSTION CHAMBER
GAS INJECTOR
SOLID PROPELLANT MOTOR
PRESSURE MEASUREMENT SECTION
NOZZLE
SAFETY HEAD
PRESSURE TRANSDUCER
SPARK PLUG FOR IGNITION OF GAS MOTOR
OXYGEN
METHANE
CASE BONDED SOLID PROPELLANT GRAIN
VIEW FROM NOZZLE

GASEOUS IGNITION OF SOLID PROPELLANT ROCKET MOTOR

FIGURE I

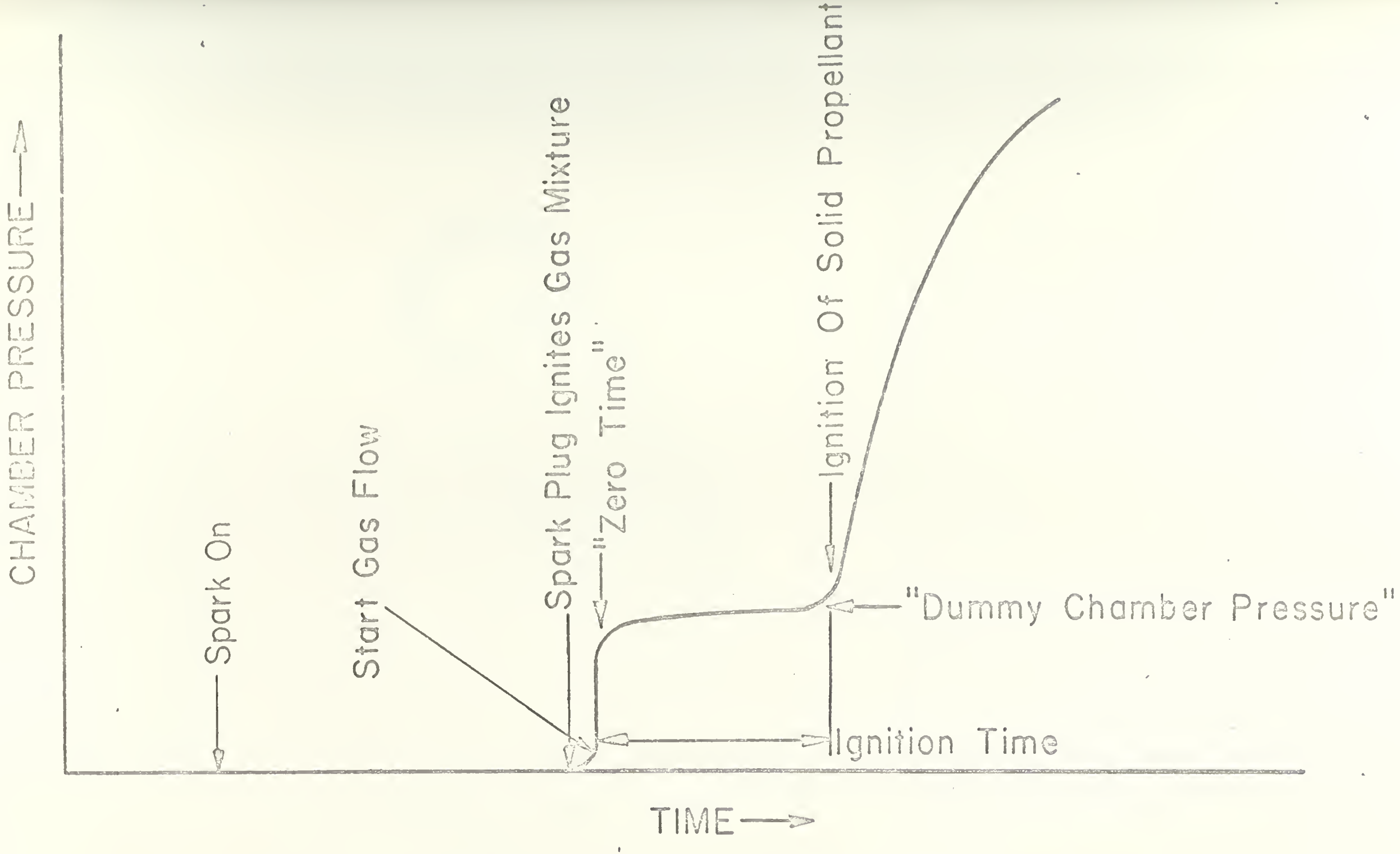

INTERPRETATION OF IDEALIZED IGNITION RECORD

FIGURE 2

FIG 3. SOLID PROPELLANT CASE-BONDED GRAIN. Upper-Grain as it appears after drilling the grain port. Lower-Grain ready to be placed in motor for firing. O-ring seal also on grain end not visible.

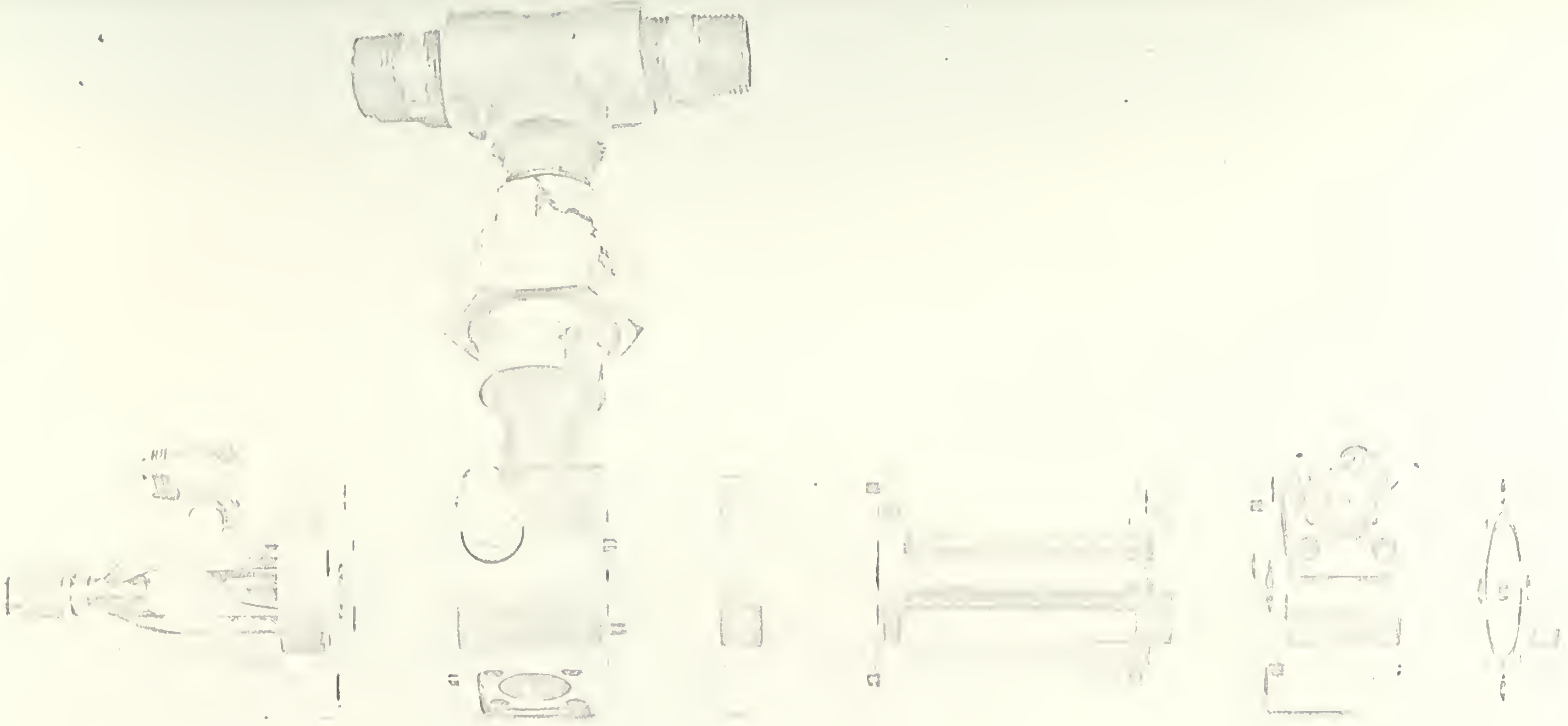

FIG 4. EXPLODED VIEW OF MOTOR. Component parts left to right: injector, gas rocket combustion chamber with spark plug and pressure safety relief connection, gas rocket nozzle, solid propellant motor casing, housing containing pressure transducer, and exit nozzle.

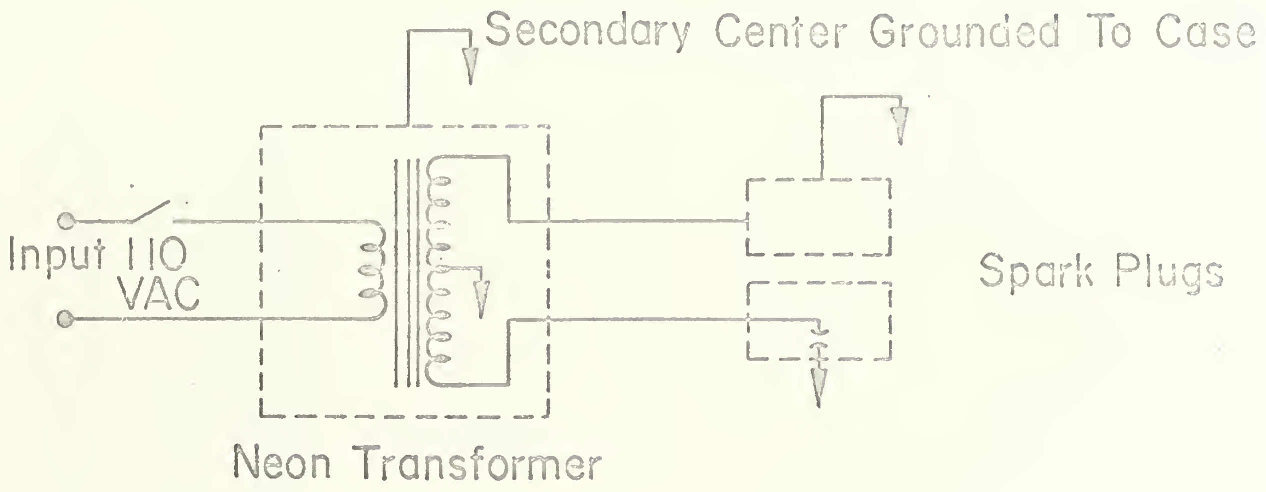
Secondary Center Grounded To Case
Input 110
VAC
Neon Transformer
Spark Plugs

CIRCUIT DIAGRAM FOR SPARK IGNITION OF GAS IGNITER
FIGURE 5

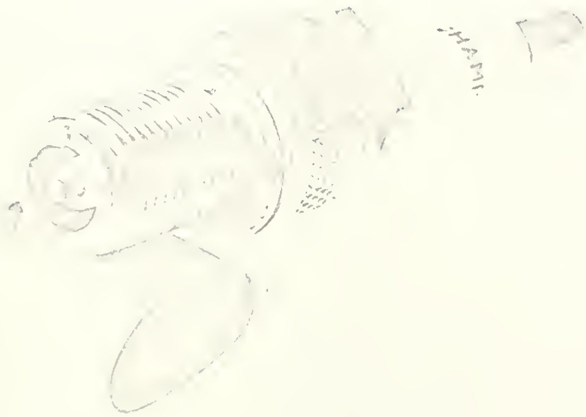

FIG 6. MODIFIED SPARK PLUG

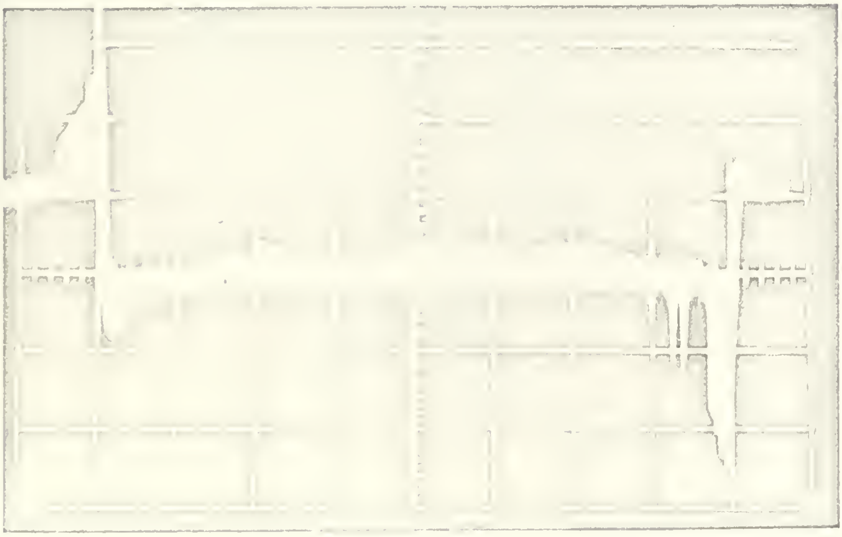

FIG 7. VOLTAGE-TIME TRACE OF SPARK PLUG GAP DURING 1/2 CYCLE OF 60 cps INPUT

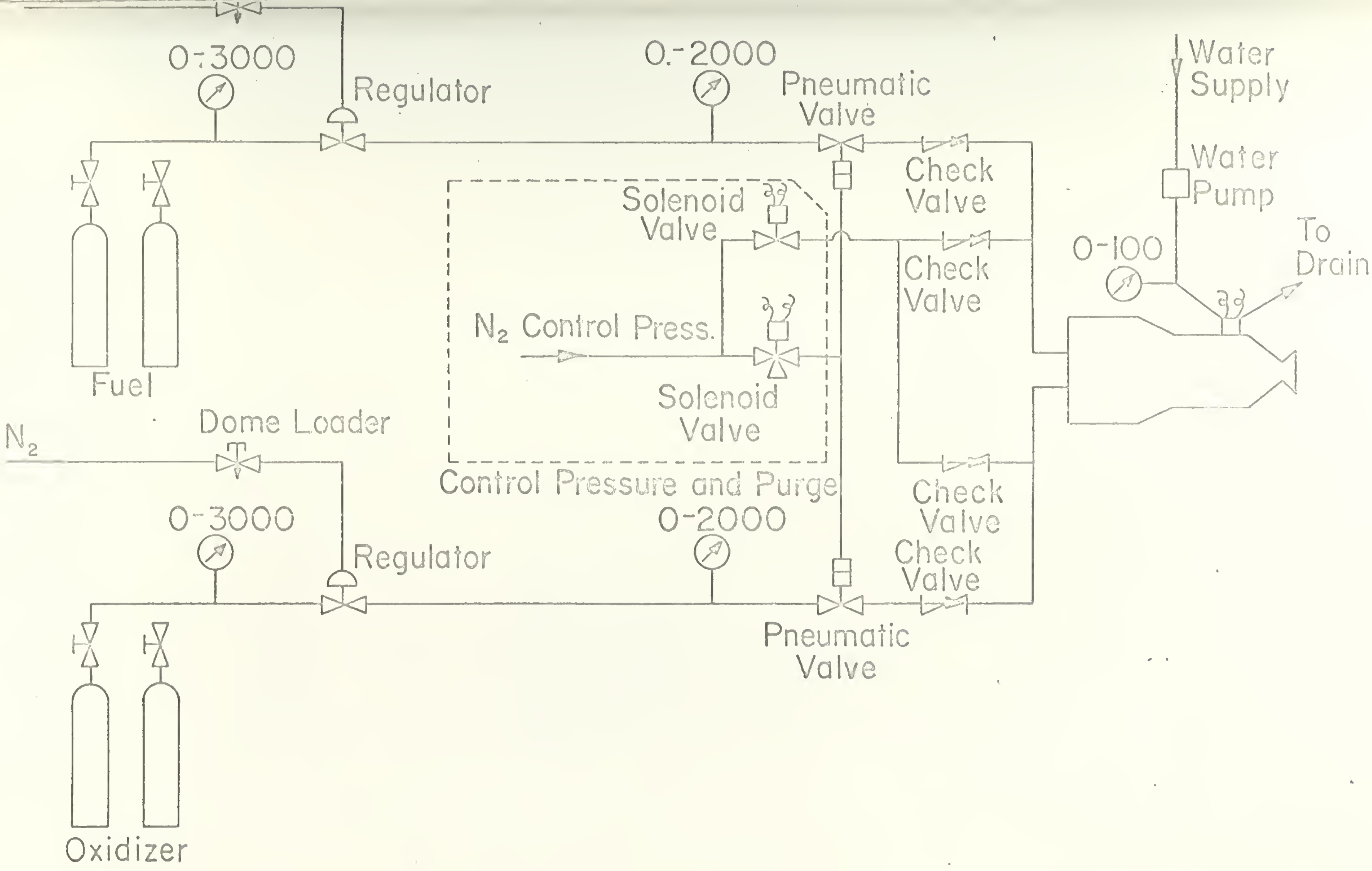

0-3000
Regulator
0-2000
Pneumatic Valve
Water Supply
Water Pump
Check Valve
Solenoid Valve
Check Valve
0-100
To Drain
N_2 Control Press.
Fuel
Solenoid Valve
Dome Loader
N_2
Control Pressure and Purge
Check Valve
0-3000
0-2000
Regulator
Check Valve
Pneumatic Valve
Oxidizer

FLOW CIRCUIT FOR IGNITER GASEOUS COMBUSTIBLES AND TRANSDUCER COOLING WATER
FIGURE 8

FIG 9. STRAIN GAGE TYPE, WATER-COOLED PRESSURE TRANSDUCER (Dynisco Corporation)

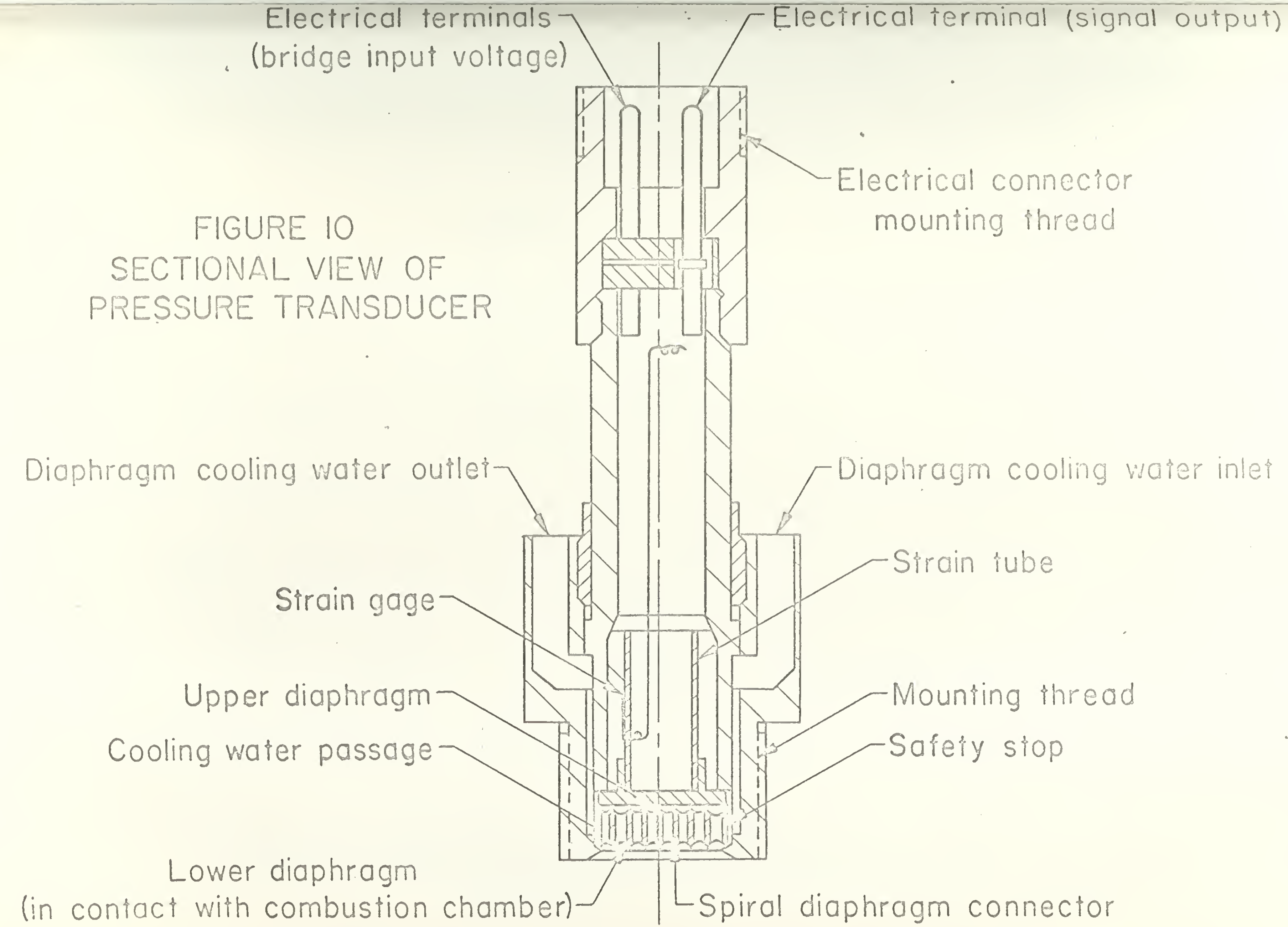

Electrical terminals
(bridge input voltage)
Electrical terminal (signal output)
Electrical connector
mounting thread
Diaphragm cooling water outlet
Diaphragm cooling water inlet
Strain tube
Strain gage
Upper diaphragm
Mounting thread
Cooling water passage
Safety stop
Lower diaphragm
(in contact with combustion chamber)
Spiral diaphragm connector

FIGURE 10
SECTIONAL VIEW OF
PRESSURE TRANSDUCER

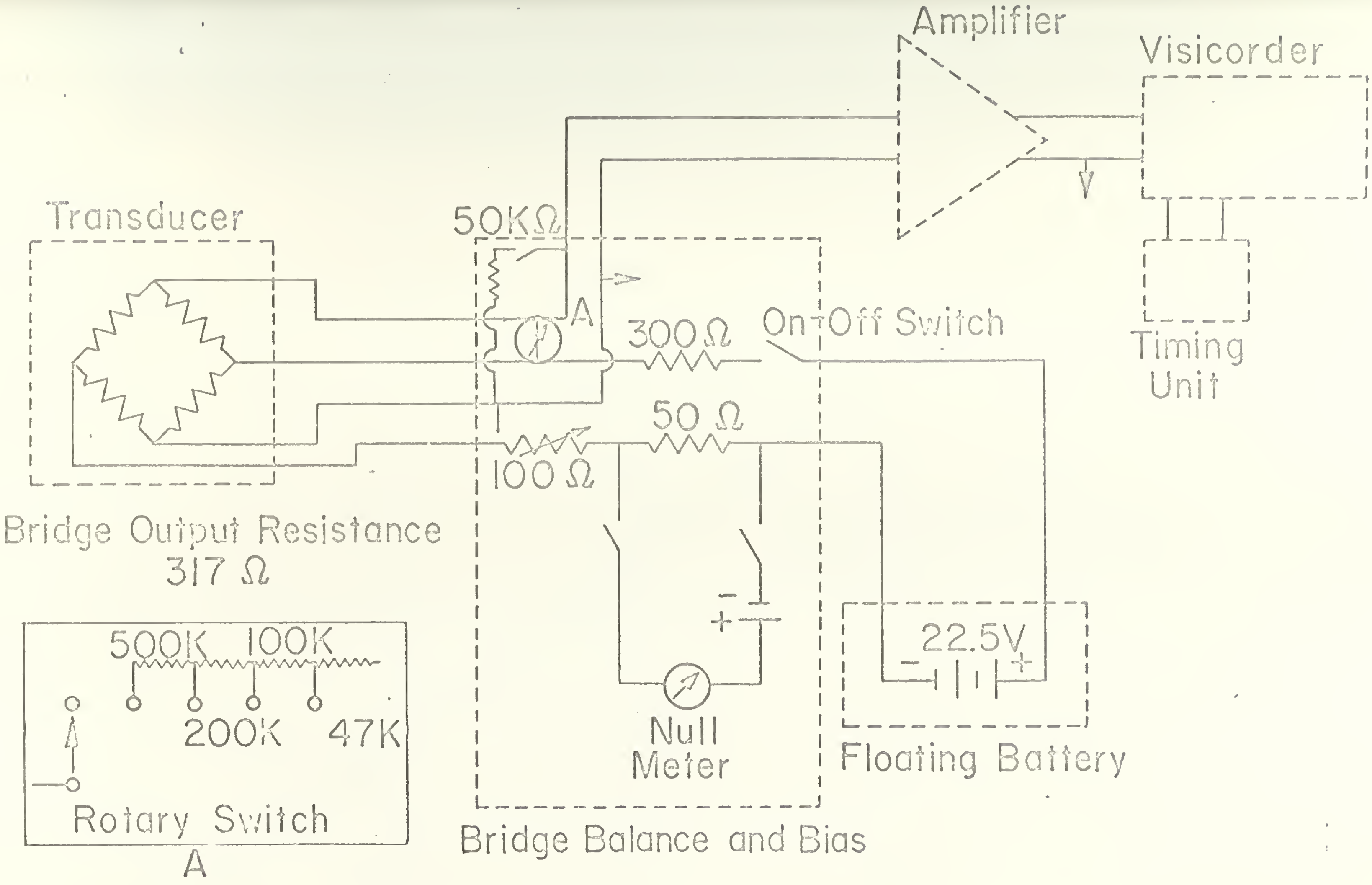
Amplifier
Visicorder
Timing Unit
Transducer
50KΩ
A
300Ω
On-Off Switch
50 Ω
100 Ω
Bridge Output Resistance 317 Ω
500K
100K
200K
47K
Rotary Switch
A
Null Meter
22.5V
−
+
Floating Battery
Bridge Balance and Bias

CIRCUIT FOR STRAIN GAGE INSTRUMENTATION
FIGURE 11

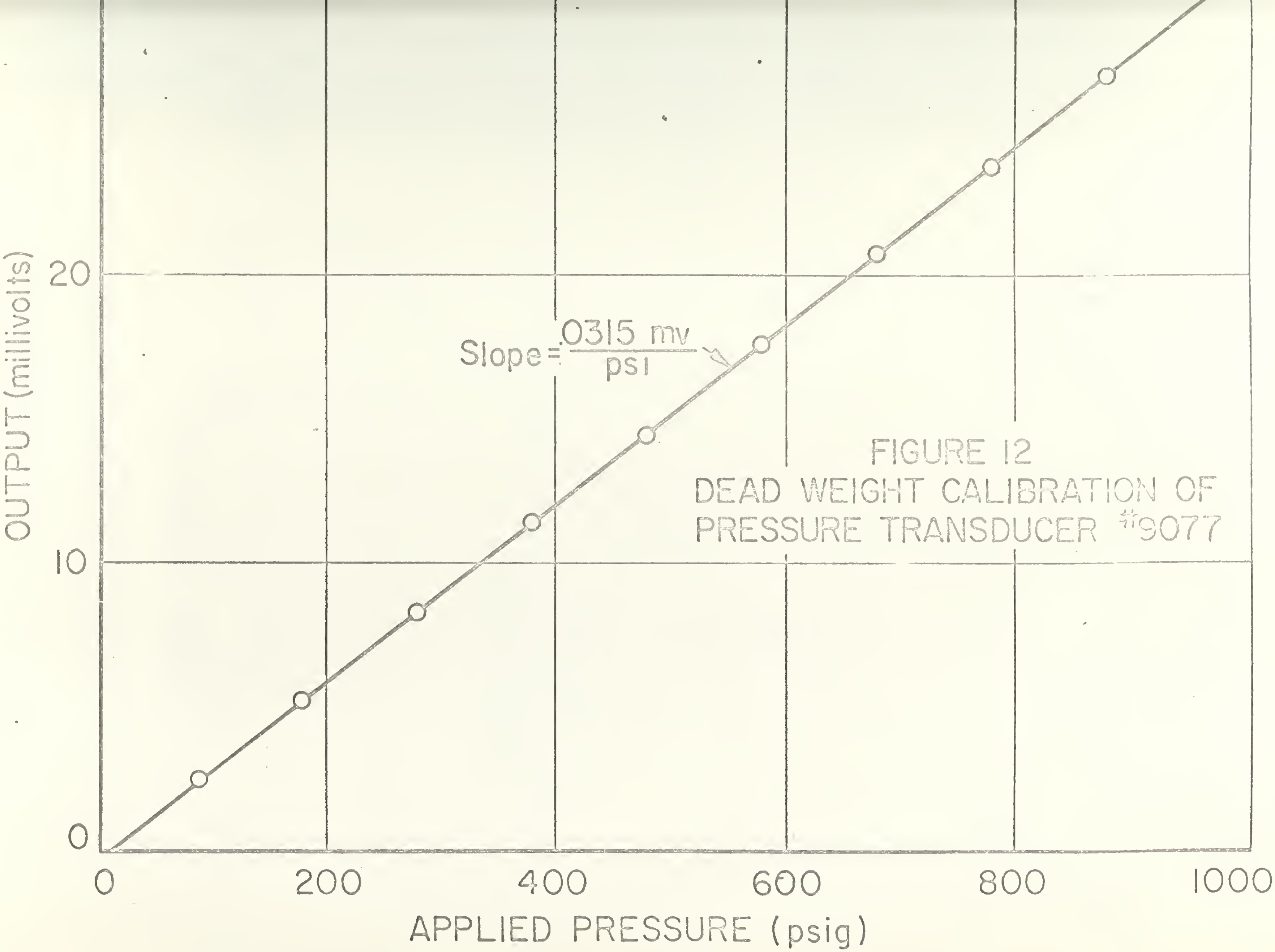

FIGURE 12
DEAD WEIGHT CALIBRATION OF
PRESSURE TRANSDUCER #9077

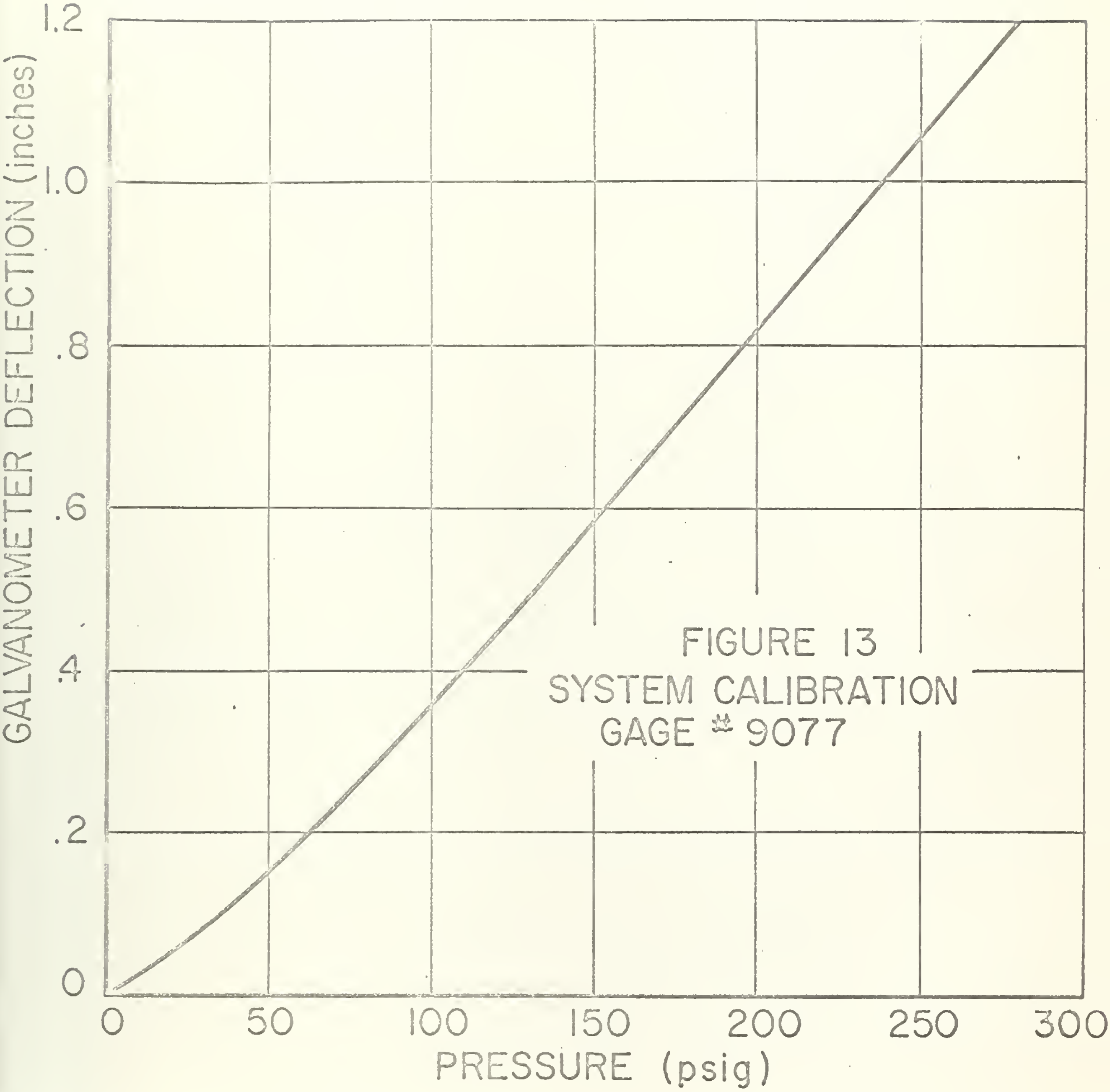
FIGURE 13
SYSTEM CALIBRATION
GAGE # 9077

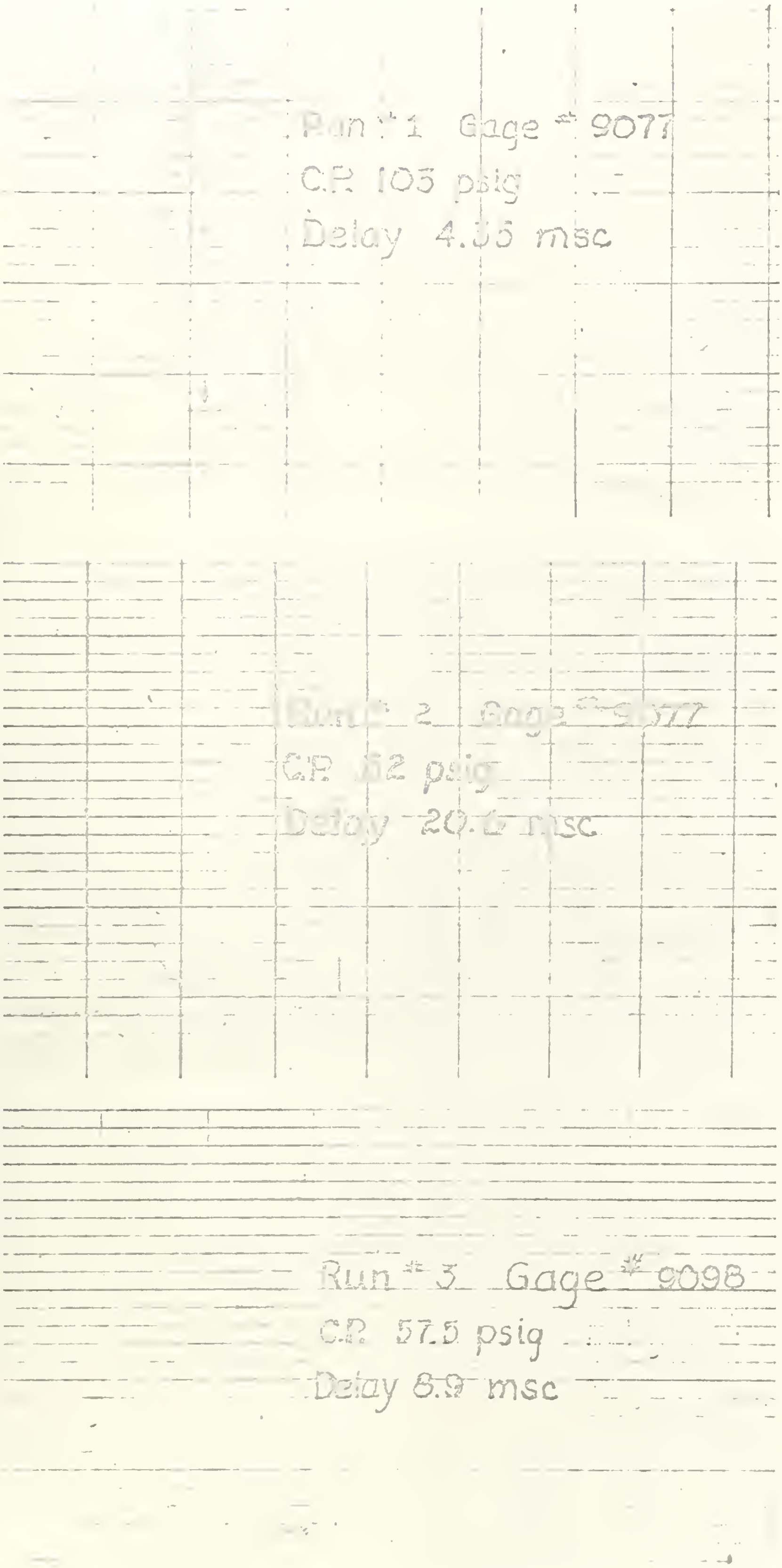

FIG 14. IGNITION PRESSURE-TIME TRACES SHOWING IGNITION DELAY

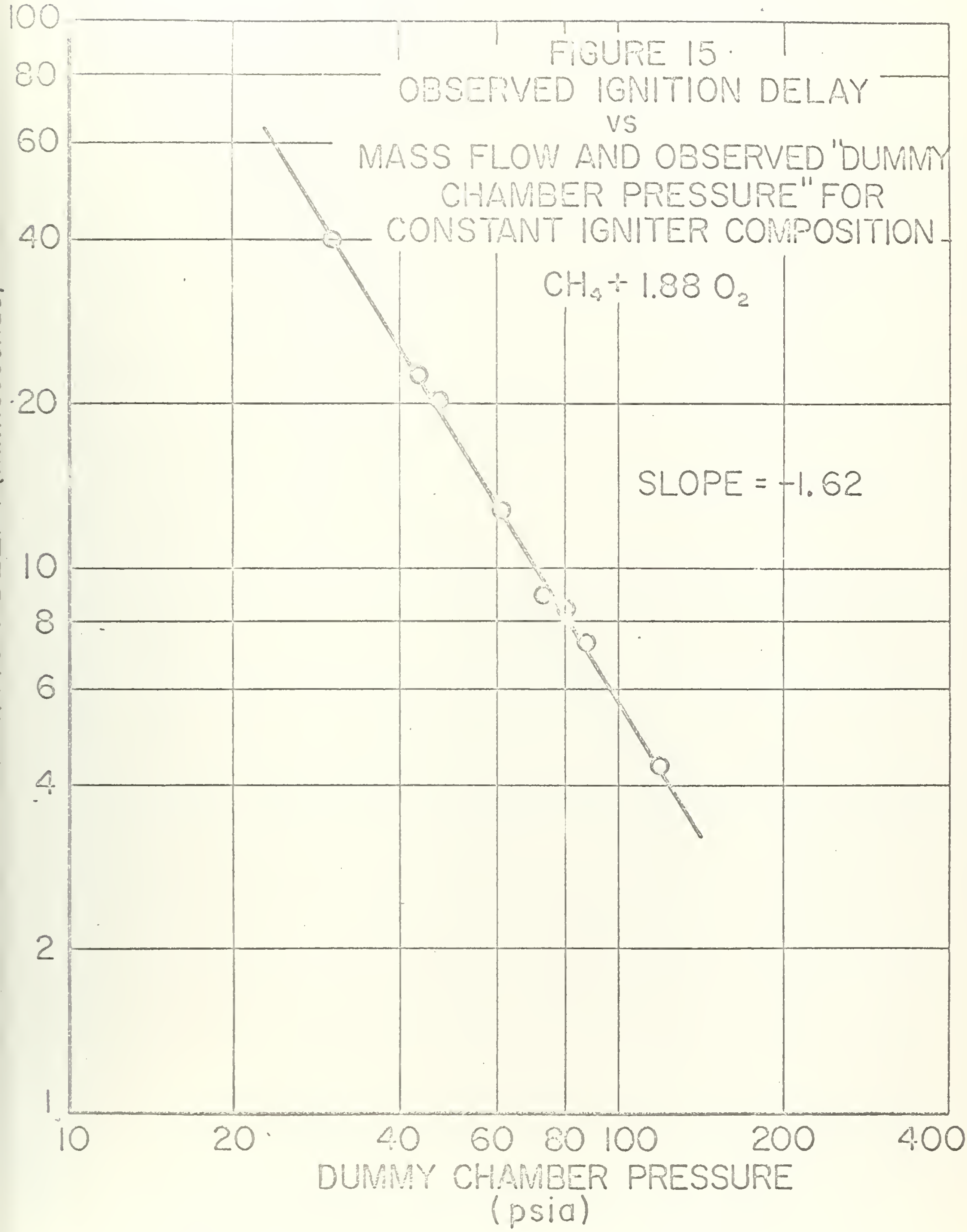

FIGURE 15
OBSERVED IGNITION DELAY
VS
MASS FLOW AND OBSERVED "DUMMY CHAMBER PRESSURE" FOR CONSTANT IGNITER COMPOSITION

$CH_4 + 1.88\ O_2$

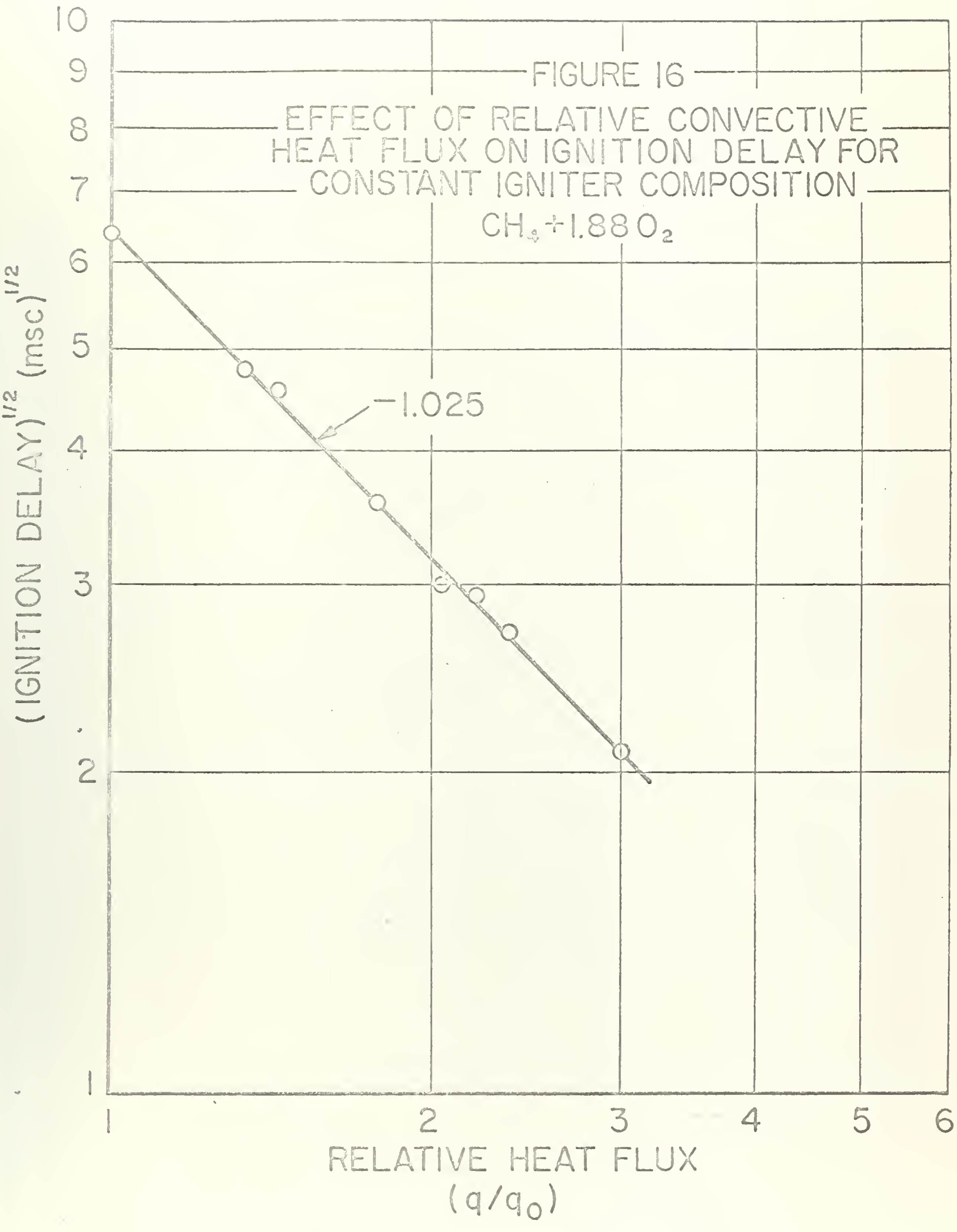

FIGURE 16

EFFECT OF RELATIVE CONVECTIVE HEAT FLUX ON IGNITION DELAY FOR CONSTANT IGNITER COMPOSITION

$CH_4 + 1.88\,O_2$

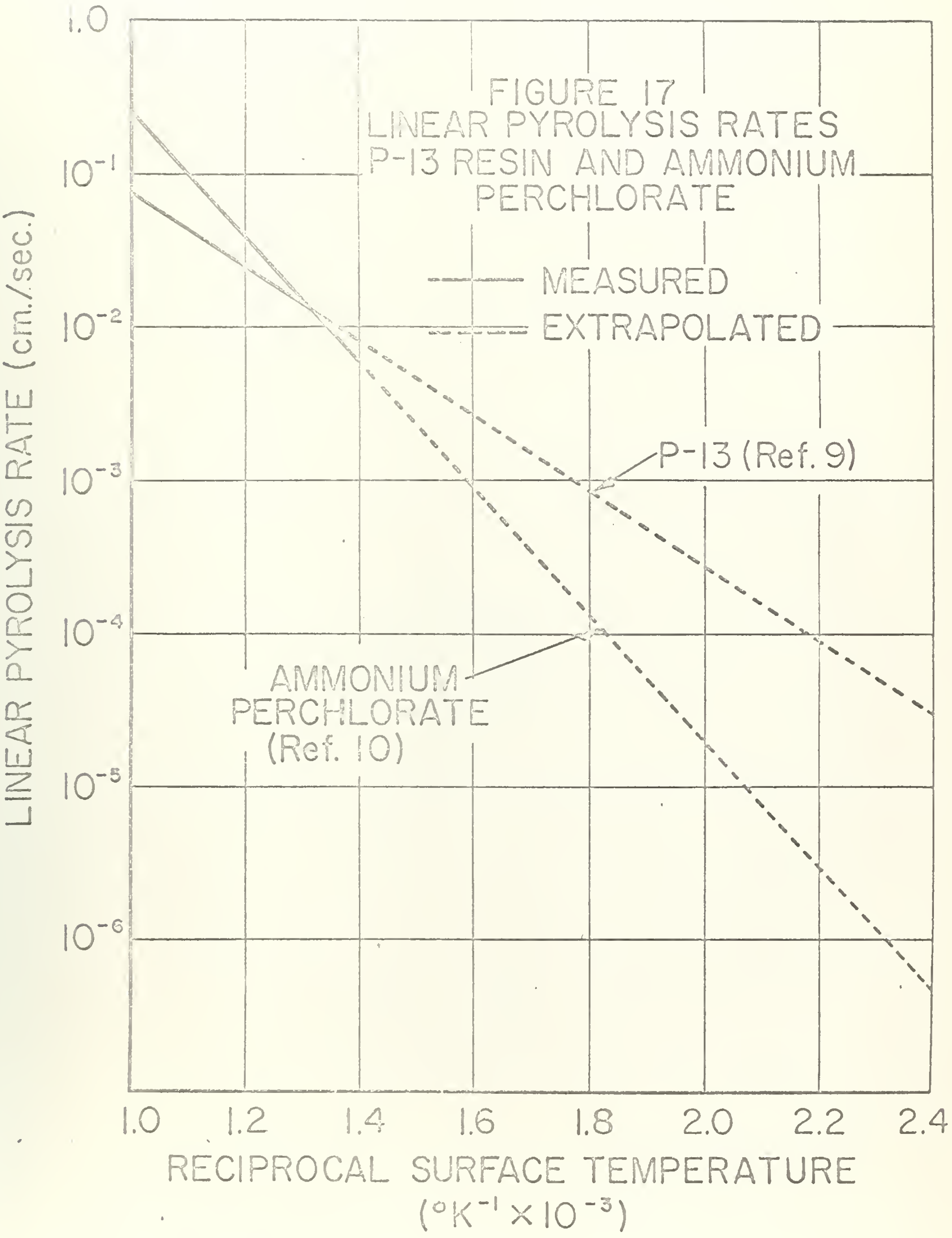

FIGURE 17
LINEAR PYROLYSIS RATES
P-13 RESIN AND AMMONIUM PERCHLORATE

FIG 18. SOLID PROPELLANT MOLD.
Upper-Exploded view of mold. Components from left to right: cap, mandril, case to which solid propellant is bonded, and base.
Lower - Assembled mold.

FIG 19. SOLID PROPELLANT CASTING APPARATUS.

thesL256
Experimental investigation of the igniti
3 2768 002 11313 6
DUDLEY KNOX LIBRARY